Second-harmonic generation in a laterally azo-bridged trimer ferroelectric liquid crystal: Phase matching in the presence of a helicoidal structure

J. Etxebarria,[1] J. Ortega,[2] C. L. Folcia,[1] Y. Zhang,[3] and C. Walker[3]
[1]*Department of Condensed Matter Physics, University of the Basque Country, UPV/EHU, 48080 Bilbao, Spain*
[2]*Department of Applied Physics II, University of the Basque Country, UPV/EHU, 48080 Bilbao, Spain*
[3]*Micron Technology Inc., 2602 Clover Basin Drive, Longmont, Colorado 80503, USA*
(Received 3 September 2012; published 27 November 2012)

Optical second-harmonic generation (SHG) has been studied in a trimer smectic C^* liquid crystal especially designed for nonlinear optical applications. The molecule has a long conjugated donor-acceptor unit that transversally links three parallel rod-shaped moieties. A strong SHG signal has been observed at a fundamental wavelength of 1369 nm even in the presence of the spontaneous helicoidal structure of the smectic C^* phase. This unusual behavior has been interpreted as due to the existence of phase matching, in which the wave vector mismatch is compensated by the wave vector of the helix. This point has been confirmed by the study of the SHG intensity versus sample thickness and light polarization characteristics. The main coefficient of the second-order susceptibility tensor of the material has been estimated to be $d_{22} = 28$ pm/V.

DOI: 10.1103/PhysRevE.86.051707 PACS number(s): 61.30.−v, 42.65.Ky, 42.70.Df

I. INTRODUCTION

It is well known that ferroelectric liquid crystals (FLCs) are potentially attractive materials from the viewpoint of nonlinear optics (NLO) [1]. FLCs with a large second-order susceptibility are a compelling alternative to inorganic and poled-polymer compounds since they offer important advantages. For example, FLCs possess inherent thermodynamically stable polar order, their polar direction can be externally controlled with an electric field, and they can be integrated with already available silicon technology on large areas, allowing for the fabrication of more complex hybrid devices.

The first approaches to the design of NLO FLCs used normal calamitic mesogens [2–8]. More recently bent-core liquid crystals have also been studied, with improved NLO efficiencies [9–12] since their bent shape allows the effective incorporation of stronger chromophores while preserving the mesogenic character.

Using an alternative idea proposed by Walba *et al.* [13] we reported a class of laterally azo-bridged H-shaped dimer FLCs [14,15] in which a disperse red (DR-1) unit transversally connects a pair of rod-shaped moieties. These materials possess an enantiotropic SmC^* phase, and second-harmonic generation (SHG) measurements of one dimer at a wavelength of 1064 nm gave a d_{22} coefficient of 17 pm/V. Continuing with this approach, a SHG investigation on the trimer shown in Fig. 1 has been recently presented [16]. Since the NLO moiety is longer than DR-1, an improved SHG efficiency far from material resonances was obtained. The SHG results show in addition some unexpected features, the most prominent of which is the appearance of a SHG signal in absence of an applied electric field.

The SHG process in helicoidal SmC^* phases was theoretically analyzed some years ago [17–19]. In particular it was shown that the helicoidal structure provides some special possibilities to achieve phase matching (PM). The same effect was reported earlier for third-harmonic generation in cholesterics [20]. The wave vector mismatch can be compensated with the wave vector of the helix similarly to what happens in the so-called quasi PM with periodically poled materials. In fact there are several possibilities for the PM. Some experimental studies carried out on this subject have shown an actual enhancement of the SHG by helicoidal distributed feedback action in SmC^* phases [21]. This is a peculiar PM process involving two counterpropagating fundamental waves and generating light in both directions with a wavelength equal to the optical pitch of the helix. As will be shown below our results can be explained in terms of two other helicoidal phase matchings (HPMs) involving waves propagating only in the forward direction. The main point of the present work is the detailed description and analysis of this phenomenon.

II. MATERIAL CHARACTERISTICS AND EXPERIMENTAL PROCEDURE

The phase sequence of the compound can be seen in Fig. 1. Despite the rather planar molecular shape, the material shows a broad SmC^* phase. Textures (Fig. 2) show the typical lines, which indicate a helicoidal structure with a pitch $p = 1.7\ \mu$m, practically constant in the SmC^* range. The helicoidal structure can easily be unwound by an electric field. Polarization measurements gave a spontaneous polarization $P_s = 27$ nC/cm^2 at 120 °C. Other characterization measurements [differential scanning calorimetry (DSC), x-ray, tilt angle, electro-optic studies] confirmed the above phase assignment [16].

The material is rather absorbing in the visible range. In fact its absorption spectrum in CH_2Cl_2 solution [16] shows a strong band in the visible range at $\lambda_0 = 572$ nm (maximum molar absorption coefficient $\varepsilon_{max} = 27\,700$ M^{-1} cm^{-1}). For this reason, the wavelength of a Nd:YAG laser (1064 nm) which is usual in SHG measurements is not a good choice in this case. Therefore, we placed a Raman-shifter crystal [$Ba(NO_3)_2$] after the Nd:YAG laser of our SHG equipment [22] to get a wavelength shifted by a second-Stokes process to 1369 nm. The material still shows some absorption at the second-harmonic wavelength 684.5 nm, though the main effect is avoided. In any case, the absorption coefficient of the

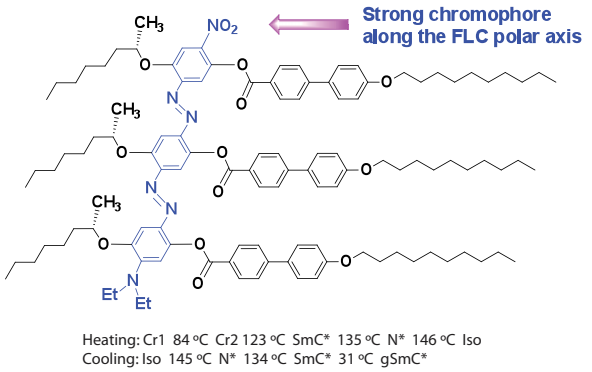

FIG. 1. (Color online) Molecular structure of the trimer incorporating a strong chromophore along its polar axis and its phase sequence according to DSC data. Cr: the crystalline state; Iso: the isotropic liquid; gSmC^*: the glassy state of the SmC^* phase.

material at 684.5 nm, extrapolated from the measurements in CH_2Cl_2 solution, is quite high, $\alpha = 0.74\ \mu m^{-1}$, and should be taken into account in the interpretation of the results.

SHG measurements were carried out at normal incidence using cells made of two glass plates treated with octadecyltriethoxysilane (ODS) to attain homeotropic orientation. One of the glasses was coated on its inner surface with two transparent indium tin oxide (ITO) electrodes parallel to each other for electric field application. The gap between electrodes was 0.1 mm. Five cells were used, with thicknesses 1, 2, 3.75, 7, and 11 μm. The material was introduced by capillarity in the isotropic phase. In all cases very good alignment was achieved in the SmC^* phase, with a uniform dark texture that became birefringent within the gap region upon field application. This fact indicates that the smectic layers are parallel to the plates and the helicoidal structure is wound or unwound depending on the absence or presence of the in-plane electric field. Typical values to unwind the helix in this homeotropic geometry are about 5 V/μm, similar to those needed for planar or unaligned samples.

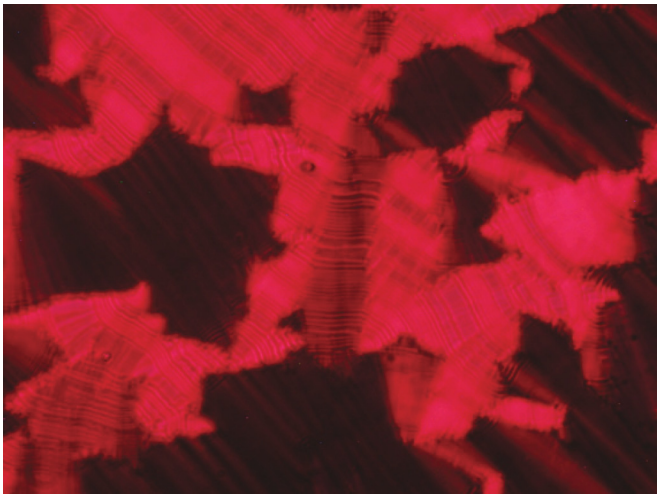

FIG. 2. (Color online) Optical textures of the trimer compound at 120 °C in a cell of thickness 6 μm. The fact that the material is switchable with electric fields of about 4 V/μm and the helix lines in the absence of a field indicate a SmC^* phase. From the distance between the lines a pitch of 1.7 μm was deduced.

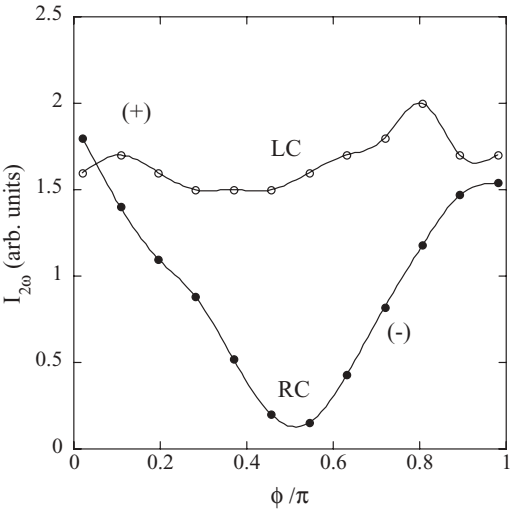

FIG. 3. SHG for different polarizations of the fundamental wave in the 11-μm thickness cell. Horizontal and vertical components have the same amplitude and a phase difference given by ϕ, i.e., the Jones vector is $\frac{1}{\sqrt{2}}\begin{pmatrix}1\\ e^{\pm i\phi}\end{pmatrix}$. Open and closed symbols correspond to the upper and lower signs, respectively. For $\phi = \pi/2$ the light is LC (plus sign) or RC (minus sign).

III. SHG RESULTS IN A HELICOIDAL SmC^* STRUCTURE

As mentioned above a strong SHG signal was observed in all the cells even before field application. These large SHG signals were obtained in practically the entire SmC^* range. Typically the SHG intensity increased with sample thickness and tended to saturate for thicknesses about 10 μm.

In general the SHG light was found to be elliptically polarized for linearly polarized fundamental light. When the polarization plane of the input light was rotated by a certain angle, the azimuth of the output light rotated by the same amount. For other polarizations of the incident light the behavior of SHG intensity is interesting, as shown in Fig. 3. The different polarizations were achieved by means of a compensator placed at 45° with respect to the plane of polarization of the incident light. As can be seen, the SHG vanishes for right circularly (RC) polarized light and remains strong for left circularly (LC) polarized light. This characteristic unambiguously indicates that the helicoidal structure plays a relevant role in the effect. This left-right asymmetry together with the large size of the SHG intensity suggests that we are observing a SHG process where a PM condition takes place and where the SmC^* helicoid is involved.

We now summarize the basic aspects of the theory for SHG in helicoidal structures [18,19]. Figure 4 shows the dispersion curves for light propagating along the helix axis of a SmC^* structure. Mode l is a coherent superposition of two Bloch waves with wave vectors $l \pm q$ where $q = 2\pi/p$ is the helix wave vector. The four curves can be calculated from the expressions [18]

$$l = \pm\left[\left(k_0^2\bar{n}^2 + q^2\right) \pm \sqrt{4k_0^2\bar{n}^2q^2 + a^4k_0^4}\right]^{1/2}, \qquad (1)$$

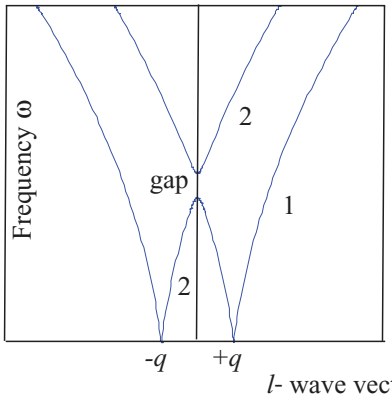

FIG. 4. (Color online) Dispersion relationship for light propagation along the helicoidal axis in a SmC* phase. Modes in branches 1 and 2 propagate in the forward direction. If the helix is positive ($q > 0$) and the anisotropy a is not too large, modes in branches 1 and 2 have essentially LC and RC polarizations, respectively, for all frequencies of practical interest. If $q < 0$ the polarizations are the opposite. These results do not apply near the gap (close to $l = 0$).

where all sign combinations are possible. Here $k_0 = \omega/c$ is the wave vector in vacuum, c the speed of light, and ω the light frequency. The parameters $\bar{n}^2$ and a^2 account for the mean refractive index and anisotropy of the material. They are related to the values of tilt angle θ and the optical dielectric tensor components parallel $\varepsilon_\parallel$ and perpendicular $\varepsilon_\perp$ to the director according to the equations

$$\bar{n}^2 = \frac{1}{2}\left[2\varepsilon_\perp + \frac{(\varepsilon_\parallel - \varepsilon_\perp)\varepsilon_\perp \sin^2\theta}{\varepsilon_\perp \sin^2\theta + \varepsilon_\parallel \cos^2\theta}\right], \quad a^2 = \bar{n}^2 - \varepsilon_\perp. \tag{2}$$

For each frequency, four modes are allowed (except in the gap region).

Modes in branches 1 and 2 have positive propagation velocities (forward propagation) and here we will restrict ourselves to these branches. For light frequencies of practical interest it can be shown that if the helix is positive ($q > 0$) the modes of branches 1 and 2 have essentially left circular (LC) and right circular (RC) polarizations, respectively. The corresponding refractive indices n_L,n_R are given approximately through the expressions

$$l - q = k_0 n_L \ \text{ branch 1}; l + q = k_0 n_R \ \text{ branch 2}. \tag{3}$$

The PM condition for SHG is realized for $\Delta l = 0$ [18,19], i.e.,

$$l(\omega) + l'(\omega) = l''(2\omega). \tag{4}$$

Here l and l' denote the l-wave vectors of the fundamental light photons that combine to produce a 2ω photon with wave vector l''. As can be seen the relation is similar to that of ordinary PM but now the expression involves Bloch (l) instead of the usual wave vectors ($k_0 n$).

A further simplification arises if the anisotropy is small, $a^2 \ll ql$. Except for terms in $O(a^4)$, all the refractive indices become equal, i.e., $n_L = n_R = \bar{n}$. Under these conditions Eq. (4) gives six different HPM possibilities that have been collected in Table I.

TABLE I. Possible HPMs for fundamental and SHG waves propagating in the forward direction. l_1,l_1' are the Bloch wave vectors for polarization LC (branch 1) and RC (branch 2) of the fundamental light. l_2,l_2' are the corresponding wave vectors for the SHG light. A positive helicoidal pitch means a right-handed helix. If the condition $n_2 > n_1$ is assumed, a right-handed helix gives rise to HPMs 1, 4, and 5.

HPM No.	Polarization combination	Wave vector conditions	Helicoidal pitch
1	LC + LC→LC	$2l_1 = l_2$	$\lambda/2(n_2 - n_1)$
2	LC + RC→LC	$l_1 + l_1' = l_2$	$\lambda/2(n_1 - n_2)$
3	RC + RC→LC	$2l_1' = l_2$	$3\lambda/2(n_1 - n_2)$
4	LC + LC→RC	$2l_1 = l_2'$	$3\lambda/2(n_2 - n_1)$
5	LC + RC→RC	$l_1 + l_1' = l_2'$	$\lambda/2(n_2 - n_1)$
6	RC + RC→RC	$2l_1' = l_2'$	$\lambda/2(n_1 - n_2)$

As can be seen, for a definite sign of the pitch and a definite sign of the dispersion only three HPMs are possible. For positive pitch and positive dispersion, two of them (HPMs 1 and 5) occur for a helicoidal pitch,

$$p = \frac{\lambda}{2(n_2 - n_1)}, \tag{5}$$

where n_2 and n_1 denote the refractive indices for the SHG and fundamental lights, respectively, and λ is the vacuum wavelength. The third HPM (HPM 4) takes place for a pitch three times larger.

Our case corresponds to Eq. (5). We give three examples as evidence to prove this point.

(i) For LC fundamental light, the resulting SHG light is also LC (HPM 1). If HPM 4 should occur then the polarization of the SHG light would be RC. In addition, provided that $n_2 > n_1$, this fact implies that the helicoidal pitch is positive, i.e., a right-handed helix (See Table I).

(ii) If the input light is linear the output SHG light is elliptical. This is explained as a coherent superposition of HPMs 1 and 5. Moreover, for a given input light, the output light polarization remains the same when rotating the sample about the helix axis. This was also experimentally observed.

(iii) For a more general polarization of the incident light, numerical calculations based on the exact theory described in Ref. [19] give the results shown in Fig. 5 [23]. Here we have assumed Eq. (5) to be valid and have checked that the result does not depend very much on the anisotropy a and the precise values of $\varepsilon_\parallel$ and $\varepsilon_\perp$. The data of Fig. 5 have been obtained with $\varepsilon_\parallel(\omega) = 2.50$, $\varepsilon_\perp(\omega) = 2.20$, $\varepsilon_\parallel(2\omega) = 4.11$, $\varepsilon_\perp(2\omega) = 3.55$, $p = +1.7\mu$m, $\theta = 20^\circ$, $\lambda = 1369$ nm, and a cell thickness $L = 11\,\mu$m. As can be seen the correspondence with the experimental points (Fig. 3) is remarkable.

If perfect HPM is achieved then Eq. (5) predicts a rather high dispersion, $n_2 - n_1 = 0.4$. This can be understood in terms of the relative proximity of 2ω to the band at 572 nm [16]. The sign of the index dispersion is assumed to be positive since at the fundamental and SHG wavelengths normal dispersion is expected. It is interesting to point out that though our results do not necessarily imply an exact HPM, the actual helicoidal pitch must be close to the HPM value. Figure 6 shows the theoretical SHG intensity as a function of the pitch for a cell of 11 μm. A

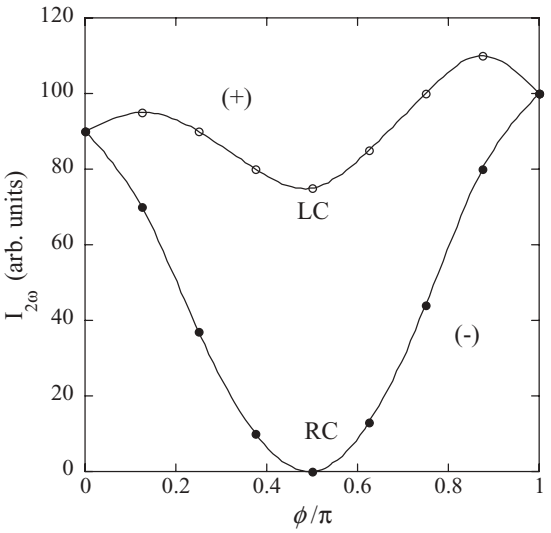

FIG. 5. Theoretical predictions for the SHG intensity at different polarizations of the fundamental light. A positive helix was assumed and SHG data were taken at the maximum of the PM peak. The Jones vector of the incident light was $\frac{1}{\sqrt{2}}\begin{pmatrix}1\\ e^{\pm i\phi}\end{pmatrix}$ with the open and closed symbols corresponding to the upper and lower signs, respectively. For $\phi = \pi/2$ the light is LC (plus sign) or RC (minus sign).

linearly polarized input light is assumed. As can be seen the width of the first SHG peak is rather small (the second peak corresponds to HPM 4). The experimental observation of an intense SHG implies then a margin for the pitch of less than 0.2 μm from the exact HPM value.

IV. MAGNITUDE OF THE SHG EFFICIENCY

A key point to identify a PM process is the study of the SHG intensity as a function of the sample thickness, which we present next, along with an estimation of the second-order susceptibility value d_{ij} of the material. The exact analysis is complicated because, besides the helix, the SHG calculations should also incorporate the existence of absorption. Here we present a simple approach that takes into account both aspects of the problem.

We will start by recalling an expression for the SHG intensity $I_{2\omega}$ in a homogeneous sample, at normal incidence

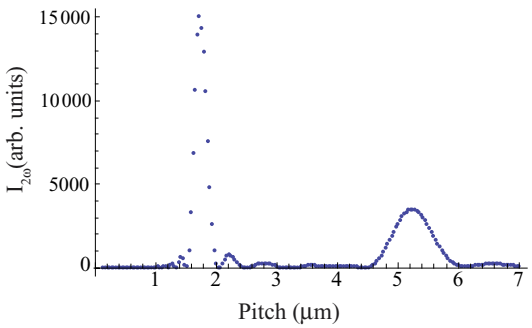

FIG. 6. (Color online) SHG versus pitch for a $L = 11$-μm-thick cell. A linearly polarized fundamental light is assumed. The HPM peak at $p = 1.7$ μm has a FWHM of 0.3 μm.

and neglecting the absorption at ω, [24]

$$I_{2\omega} = Cd_{\text{eff}}^2 L^2 e^{-\alpha L/2}\frac{\sin^2(\Delta kL/2)+\sinh^2(\alpha L/4)}{(\Delta kL/2)^2+(\alpha L/4)^2}, \quad (6)$$

where C is a constant, α the absorption coefficient of SHG light, d_{eff} an effective nonlinear coefficient depending on the input and output polarizations, and $\Delta kL/2$ is the phase mismatch between second-harmonic and fundamental lights. In the presence of a helicoidal structure it seems reasonable to expect the validity of Eq. (6) except that now Δl should appear instead of Δk. For HPM, since $\Delta l = 0$, we will have

$$I_{2\omega} = Cd_{\text{eff}}^2 L^2 e^{-\alpha L/2}\frac{\sinh^2(\alpha L/4)}{(\alpha L/4)^2}. \quad (7)$$

If the absorption is dominant, as in our case, the SHG intensity is constant for thicknesses larger than a relatively short L (of the order of, let us say, $10/\alpha$). However, in the hypothetical case of a nonabsorbing material we have checked numerically that the intensity is proportional to L^2. In order to highlight this fact, in Fig. 7 a fit of the SHG intensity for LC polarized fundamental light divided by the absorption dependent factor $F(L) = e^{-\alpha L/2}\frac{\sinh^2(\alpha L/4)}{(\alpha L/4)^2}$ versus L^2 is depicted. As can be seen a straight line is obtained in agreement with Eq. (7). The only fitting parameter is the proportionality constant Cd_{eff}^2. The absorption coefficient is taken, $\alpha = 0.74\,\mu\text{m}^{-1}$ (from the extrapolation of the absorption measurements in CH_2Cl_2 solution). The good fit gives us some confidence on our hypothesis, at least if the HPM condition holds. The constant C can be obtained by comparison of $I_{2\omega}$ with the SHG signal of quartz $I_{2\omega}^{\text{quartz}}$. Using a y-cut quartz plate and the ordinary + ordinary→ordinary SHG conversion we have $I_{2\omega}^{\text{quartz}} = 4Cd_{11}^2/(\Delta k^{\text{quartz}})^2$ for the maximum of the first Maker fringe. Taking $d_{11} = 0.4$ pm/V for quartz at 1369 nm we obtain $d_{\text{eff}} = 10$ pm/V for the trimer material.

d_{eff} is the effective susceptibility for the process that transforms two LC ω photons into one 2ω LC photon when

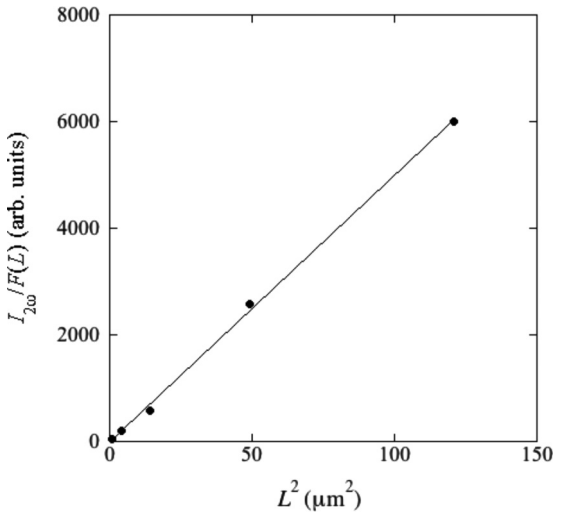

FIG. 7. SHG intensity divided by the factor $F(L) = \exp(-\alpha L/2)\frac{\sinh^2(\alpha L/4)}{(\alpha L/4)^2}$ as a function of the square of the sample thickness at 120 °C at zero field. The fundamental light had a LC polarization. The straight line is a fit to Eq. (7) with the slope (Cd_{eff}^2) as the only free parameter.

the SmC^* helix is wound. This susceptibility is related in a rather complicated fashion with the four independent d_{ij} coefficients of the unwound structure [18]. However, assuming that, because of the molecular design, d_{22} is much larger than the rest (y is the axis parallel to the spontaneous polarization of the unwound structure) a simple expression for d_{eff} results [16], $d_{\text{eff}} = d_{22}/(\sqrt{2})^3$. This gives $d_{22} = 28$ pm/V, which is even higher than that reported for the dimer compound [14,15]. This considerable size for an NLO susceptibility is only a relative surprise because, as previously pointed out, the conjugation length of the chromophore is crucial for the magnitude of the hyperpolarizability. Though the coefficient is somewhat resonance enhanced, the obtained value indicates the efficacy of the employed chemical design in achieving high performance NLO FLCs.

V. CONCLUSIONS

In summary, we have studied the SHG of a FLC especially designed for NLO applications. Despite the planar molecular shape, the material possesses a SmC^* phase with a helicoidal structure. It has been shown that a SHG signal is observed even in the absence of any electric field. The phenomenon has been identified with a PM in which the helicoidal structure plays an important role. Finally we have estimated $d_{22} = 28$ pm/V at 1369 nm, which is a value enabling viable applications (e.g., the NLO coefficient for widely used commercial periodically poled lithium niobate (PPLN) is $d_{33} = 27$ pm/V).

ACKNOWLEDGMENTS

This research was supported by CICYT-FEDER of Spain-UE (Contract No. MAT2009-14636-CO3) and the Basque Country Government (Project No. GI/IT-449-10). Y.Z. and C.W. would like to thank the NSF (USA) for support through Grants No. OII-0539835 and No. IIP-0646460 to Displaytech, Inc. (now part of Micron Technology Inc.).

[1] Y. Zhang and J. Etxebarria, in *Liquid Crystals Beyond Displays*, edited by Q. Li (Wiley, Hoboken, NJ, 2012), pp. 111–156.
[2] N. M. Shtykov, M. I. Barnik, L. A. Beresnev, and L. M. Blinov, Mol. Cryst. Liq. Cryst. **124**, 379 (1985).
[3] A. Taguchi, Y. Ouchi, H. Takezoe, and A. Fukuda, Jpn. J. Appl. Phys. **28**, L997 (1989).
[4] J. Y. Liu, M. G. Robinson, K. M. Johnson, D. M. Walba, M. B. Ros, N. A. Clark, R. Shao, and D. J. Dorovski, J. Appl. Phys. **70**, 3426 (1991).
[5] K. Schmitt, R.-P. Herr, M. Schadt, J. Funfschilling, R. Buchecker, X. H. Chen, and C. Benecke, Liq. Cryst. **14**, 1735 (1993).
[6] P. Espinet, J. Etxebarria, C. L. Folcia, J. Ortega, M. B. Ros, and J. L. Serrano, Adv. Mater. **8**, 745 (1996).
[7] J. Ortega, C. L. Folcia, J. Etxebarria, M. B. Ros, and J. A. Miguel, Liq. Cryst. **23**, 285 (1997).
[8] M. Trollsås, C. Orrenius, F. Sahlén, U. W. Gedde, T. Norin, A. Hult, D. Hermann, P. Rudquist, L. Komitov, S. T. Lagerwall, and J. Lindström, J. Am. Chem. Soc. **118**, 8542 (1996).
[9] F. Kentischer, R. MacDonald, P. Warnick, and G. Heppke, Liq. Cryst. **25**, 341 (1998).
[10] F. Araoka, J. Thisayukta, K. Ishikawa, J. Watanabe, and H. Takezoe, Phys. Rev. E **66**, 021705 (2002).
[11] I. C. Pintre, N. Gimeno, J. L. Serrano, M. B. Ros, I. Alonso, C. L. Folcia, J. Ortega, and J. Etxebarria, J. Mater. Chem. **17**, 2219 (2007).
[12] I. C. Pintre, J. L. Serrano, M. B. Ros, J. Martinez-Perdiguero, I. Alonso, J. Ortega, C. L. Folcia, J. Etxebarria, R. Alicante, and B. Villacampa, J. Mater. Chem. **20**, 2965 (2010).
[13] D. M. Walba, D. J. Dyer, P. L. Cobben, T. Sierra, J. A. Rego, C. A. Liberko, R. Shao, and N. A. Clark, Ferroelectrics **179**, 211 (1996).
[14] Y. Zhang, J. Martinez-Perdiguero, U. Baumeister, C. Walker, J. Etxebarria, M. Prehm, J. Ortega, C. Tschierske, M. J. O'Callaghan, A. Harant, and M. Handschy, J. Am. Chem. Soc. **131**, 18386 (2009).
[15] J. Martinez-Perdiguero, Y. Zhang, C. Walker, J. Etxebarria, C. L. Folcia, J. Ortega, M. J. O'Callaghan, and U. Baumeister, J. Mater. Chem. **20**, 2965 (2010).
[16] Y. Zhang, J. Ortega, U. Baumeister, C. L. Folcia, G. Sanz-Enguita, C. Walker, S. Rodriguez-Conde, J. Etxebarria, M. J. O'Callaghan, and K. More, J. Am. Chem. Soc. **134**, 16298 (2012).
[17] V. A. Belyakov and N. V. Shipov, Phys. Lett. **86A**, 94 (1981).
[18] I. D. Olenik and M. Copic, Phys. Rev. E **56**, 581 (1997).
[19] H. Hoshi, D. H. Chung, K. Ishikawa, and H. Takezoe, Phys. Rev. E **63**, 056610 (2001).
[20] J. W. Shelton and Y. R. Shen, Phys. Rev. A **5**, 1867 (1972).
[21] J. G. Yoo, S. W. Choi, H. Hoshi, K. Ishikawa, H. Takezoe, and M. Schadt, Jpn. J. Appl. Phys. **36**, L1168 (1997).
[22] N. Pereda, C. L. Folcia, J. Etxebarria, J. Ortega, and M. B. Ros, Liq. Cryst. **24**, 451 (1998).
[23] Numerical calculations were carried out using a MATHEMATICA package.
[24] W. H. Herman and L. M. Hayden, J. Opt. Soc. Am. B **12**, 416 (1995).